

# Electronic and Structural Properties of $C_{36}$ Molecule

Xiaoqing Yu<sup>1,2</sup>, Congjun Wu<sup>1,3</sup>, Chui-lin Wang<sup>2</sup>, and Zhao-Bin Su<sup>3</sup>

<sup>1</sup> *Department of Physics, Peking University*

<sup>2</sup> *China Center of Advanced Science and Technology(World Laboratory),  
P.O. Box 8730, Beijing 100080, China*

<sup>3</sup> *Institute of Theoretical Physics, Chinese Academy of Sciences,  
P.O. Box 2735, Beijing 100080, China*

## Abstract

The extended SSH model and Bogoliubov-de Gennes(BdG) formalism are applied to investigate the electronic properties and stable lattice configurations of  $C_{36}$ . We focus the problem on the molecule's unusual  $D_{6h}$  symmetry. The electronic part of the Hamiltonian without Coulomb interaction is solved analytically. We find that the gap between HOMO and LUMO is small due to the long distance hopping between the 2nd and 5th layers. The charge densities of HOMO and LUMO are mainly distributed in the two layers, that causes a large splitting between the spin triplet and singlet excitons. The differences of bond lengths, angles and charge densities among the molecule and polarons are discussed.

**Key words:**  $C_{36}$ , SSH model,  $D_{6h}$  symmetry

**Contact Author:** Xiaoqing Yu

**E-mail:** xqyu@students.uiuc.edu

## I. INTRODUCTION

Recently, a new member of fullerenes,  $C_{36}$ , was synthesized by arc-discharge method and purified in bulk quantities [1]. Up to now, it is the smallest fullerene ever discovered. The  $C_{36}$  molecule is more curved than  $C_{60}$  because of the adjacent pentagonal rings and the small number of carbon atoms [1]. This feature suggests stronger electron-phonon interaction and possible higher superconducting transition temperatures in the alkali-doped  $C_{36}$  solids than those of  $C_{60}$  [2]. The Solid-State Nuclear Magnetic Resonant experiment suggested that the most favorable configuration of  $C_{36}$  molecule has  $D_{6h}$  symmetry [1]. This confirmed the results of the early *ab initio* pseudopotential density functional calculations [3], which indicated that the  $D_{6h}$  structure is one of the most energetically favorable structures among several possibilities.

Looked in a direction perpendicular to the six-fold axis(Fig.1), the molecule is composed of six parallel layers. On each layer, six carbon atoms lie at the vertexes of a hexagon. The edges of the hexagons of the 1st, 2nd, 5th, 6th layers are parallel, while those of the two hexagons in the middle two layers are turned by an angle of  $30^\circ$ . In addition to this special structure, the six-fold principal axis is distinct form the ordinary five-fold principal axis in the cases of  $C_{60}$  and  $C_{70}$  and little attention has been paid to it. In this paper, we discuss both the electronic and structural properties of  $C_{36}$  molecule, emphasizing the interesting properties brought by this unusual  $D_{6h}$  symmetry.

We employ a simple and elegant model , extended SSH model, which is successful in treating  $C_{60}$  and  $C_{70}$  [4,5]. The BdeG formalism is performed to obtain the stable lattice configuration and the corresponding electronic states self-consistently. The electronic part of Hamiltonian without Coulomb interaction can be solved analytically by methods of group theory. We find that the electron densities of  $HOMO(B_{1u})$  and  $LUMO(B_{2g})$ , are zero at the two middle layers. Furthermore, the HOMO and LUMO are mainly confined in the 2nd and 5th layers with a possibility of 90%. The gap between them is considerably small, compared to that of  $C_{60}$  and  $C_{70}$ , because the splitting of HOMO and LUMO is due to

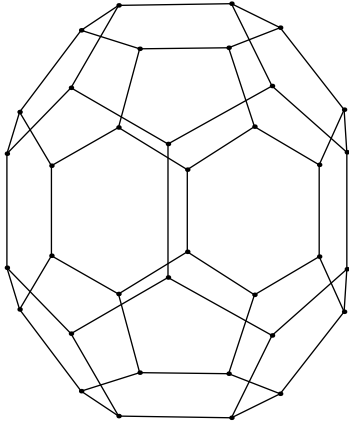


FIG. 1. The geometrical figure of  $C_{36}$  molecule.

a long-distance hopping in our case. We find the large splitting of the triplet and singlet excitons due to more localized HOMO and LUMO in comparison with  $C_{60}$  and  $C_{70}$ . As a result, the triplet exciton's energy is very small and possible experiments are suggested to test this phenomenon.

The geometrical figures of  $C_{36}$  molecule and polarons are discussed and bond lengths and angles are calculated. The charge density on each layer are given. We find that the differences of charge densities among polarons and molecule are mainly in the 2nd and 5th layers.

The following sections are arranged as: in Sec. II, the extended SSH model is introduced; in Sec. III, we analytically solve the electronic part of the Hamiltonian without Coulomb interaction; in Sec. IV, the whole Hamiltonian is solved self-consistently; in Sec. V, results and discussions are presented; and conclusions are made in the final section.

## II. MODEL

The Hamiltonian of the extended SSH model to the  $C_{36}$  molecule is written as:

$$H = H_0 + H_{int} + H_{elas} \quad (1)$$

The first term  $H_0$  of Eq.(1) is the hopping term of  $\pi$ -electrons.

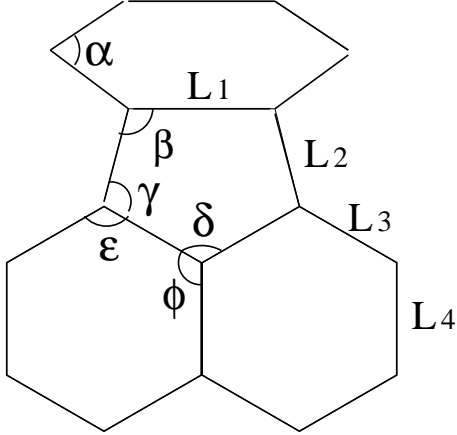


FIG. 2. The geometrical figure of C<sub>36</sub> molecule.

$$H_0 = - \sum_{\langle i,j \rangle} [t_0 - \alpha(l_{ij} - l_0)](c_{i\sigma}^\dagger c_{j\sigma} + h.c.) - \sum'_{\langle i,j \rangle} t_1(c_{i\sigma}^\dagger c_{j\sigma} + h.c.) - \sum''_{\langle i,j \rangle} t_2(c_{i\sigma}^\dagger c_{j\sigma} + h.c.) \quad (2)$$

where the three terms describe hopping between the nearest neighbors, the next nearest neighbors and the third neighbors respectively, with the corresponding hopping integrals  $t_0$ ,  $t_1$  and  $t_2$ . The influence of electron-phonon coupling is only included in the first term of  $H_0$ , since those of the last two terms are much smaller than  $t_0$ . The third term is important here because it changes the accidental degeneracy of HOMO and LUMO states, which will be explained in the next section. The larger distance terms are neglected, as they are small and do not bring any new effects.

The second term of Eq.(1) is the screened Coulomb interaction expressed in the Hubbard model.

$$H_{int} = U \sum_i n_{i\uparrow} n_{i\downarrow} + V \sum_{\langle i,j \rangle, \sigma, \sigma'} n_{i\sigma} n_{j\sigma'} \quad (3)$$

where  $U$  is the strength of the on-site interaction, and  $V$  is that between the nearest neighbors.

The third term of Eq.(1) is the elastic energy of the lattice. This term is composed of three parts,

$$H_{elas} = \frac{1}{2} K_1 \sum_{\langle i,j \rangle} (l_{ij} - l_0)^2 + \frac{1}{2} K_2 \sum_i d\theta_{i5}^2 + \frac{1}{2} K_3 \sum_i d\theta_{i6}^2, \quad (4)$$

where the first part describes the spring energy of bond-length terms, and the next two terms describe the spring energy of the angular terms.  $K_i (i = 1 \text{ to } 3)$  are the elastic constants for these different kinds of lattice vibrations.  $d\theta_{i5}, d\theta_{i6}$  are bond angle deviations from the original angle  $108^\circ, 120^\circ$ . e.g.  $d\theta_{i5} = \theta_{i5} - 108^\circ$ . The first summation is taken up over all nearest pairs. The second is of all interior angles of pentagons. And the third is of all interior angles of hexagons.

Since there are no enough experiment data to determine the semiempirical parameters, we set the values in the scope of fullerenes such as  $C_{60}$  and  $C_{70}$  which can produce reasonable results. We adjust them to give the gap between HOMO and LUMO and the bond length consistent with those of the pseudopotential density functional approach. We take  $t_0 = 2.5\text{eV}$ ,  $\alpha = 5.6\text{eV}/\text{\AA}$ ,  $L_0 = 1.55\text{\AA}$ ,  $K_1 = 47\text{eV}/\text{\AA}^2$ ,  $K_2 = 8\text{eV}/\text{rad}^2$ ,  $K_3 = 7\text{eV}/\text{rad}^2$ ,  $t_1 = 16.8\%t_0$ . In fact, the particular values, except for the value of  $t_2$ , would not affect the physics too much. Based on the calculation of the third-nearest  $\pi$ -orbit integral,  $t_2$  was estimated to be  $0.111t_0$ .

### III. ANALYTICAL RESULT OF THE ELECTRONIC HAMILTONIAN WITHOUT COULOMB INTERACTION

Fully exploiting the high  $D_{6h}$  symmetry, we solve  $H_0$  algebraically as in the case of  $C_{60}$  [6,7]. For simplicity, we temporarily ignore  $t_1$  and  $t_2$  terms and will discuss their effects in detail later. The thirty-six  $\pi$  orbits form a  $36 \times 36$  representation of the  $D_{6h}$  group. It can be reduced into the sum of following irreducible representations:

$$\{3A_{1g} \oplus B_{1g} \oplus 2B_{2g} \oplus 3E_{1g} \oplus 3E_{2g}\} \oplus \{2B_{1u} \oplus 3A_{2u} \oplus B_{2u} \oplus 3E_{1u} \oplus 3E_{2u}\} \quad (5)$$

The even-order axis  $C_6$  brings properties different from those odd-order axis  $C_5$  characterized in  $C_{60}$  and  $C_{70}$ , in the way that it has 1-D representations of kind B.

We reduce this problem by  $D_{6h}$ 's subgroup  $C_{6h}$ , using the quantum number  $m (= 0, \pm 1, \pm 2, 3)$  which corresponds to the irreducible representation of  $C_{6h}$ , and  $P (= \pm 1)$  to parity. The thirty-six  $\pi$  orbits are recombined as:

TABLE I. The analytical solution of  $H_0$  without  $t_1$  and  $t_2$  terms.

m,p	E(eV)	$c_{mp,1}$	$c_{mp,2}$	$c_{mp,3}$
0, +(A <sub>1g</sub> )	-9.51	0.581	0.574	0.578
	-5.74	0.791	-0.232	-0.566
	5.57	0.190	-0.786	0.589
0, -(A <sub>2u</sub> )	-8.43	0.816	0.504	0.284
	-3.53	-0.565	0.589	0.578
	8.43	-0.124	0.632	-0.765
$\pm 1, + (E_{1g})$	-6.28	0.647	0.654	$0.340 \pm 0.196i$
	-1.60	0.744	-0.428	$-0.445 \mp 0.257i$
	7.66	$0.145 \mp 0.084i$	$-0.540 \pm 0.312i$	0.763
$\pm 1, - (E_{1u})$	-8.09	$0.329 \mp 0.190i$	$0.534 \mp 0.308i$	0.690
	-3.25	0.882	-0.015	$-0.409 \mp 0.236i$
	4.97	-0.281	0.787	$-0.476 \mp 0.275i$
$\pm 2, + (E_{2g})$	-5.44	$0.096 \mp 0.169i$	$0.289 \mp 0.501i$	0.792
	0.269	0.573	0.589	$-0.285 \mp 0.494i$
	5.40	0.796	-0.565	$0.108 \pm 0.187i$
$\pm 2, - (E_{2u})$	-3.07	0.379	0.819	$0.216 \pm 0.374i$
	3.20	0.727	0.026	$-0.343 \mp 0.595i$
	6.25	$0.287 \mp 0.496i$	$-0.287 \pm 0.497i$	0.585
3, +(B <sub>2g</sub> )	-1.13	0.357	0.934	0
	(B <sub>1g</sub> )	3.08	0	0
	(B <sub>2g</sub> )	7.73	0.934	-0.357
3, -(B <sub>2u</sub> )	-3.08	0	0	1
	(B <sub>1u</sub> )	-1.13	0.357	0.934
	(B <sub>1u</sub> )	7.73	0.934	-0.357

$$|\Psi_{mp}^{(l)}\rangle = \sum_i \eta^{mi} \{|l, i\rangle + P|7-l, i\rangle\}. \quad (6)$$

where  $|l, i\rangle$  represents the  $i$ th ( $i = 1 \sim 6$ ) carbon atom's  $\pi$  orbit in the  $l$ th layer. Here  $l$  is only ranged for 1 to 3, and  $\eta = e^{i\pi/3}$

The energy eigenstate wavefunction  $\Phi_{mp}^l$  can be expanded with these base vectors.

$$\Phi_{mp}^i = \sum_{l=1,3} c_{mp,l}^i \Psi_{mp}^l \quad (7)$$

Consequently,  $H_0$  can also be reduced to  $3 \times 3$  matrices in the subspace which is spanned by the new bases:

$$H_{mp} = \begin{bmatrix} -t_a(\eta^{-m} + \eta^m) & -t_b & 0 \\ -t_b & 0 & -t_c(1 + \eta^{-m}) \\ 0 & -t_c(1 + \eta^m) & -t_d P \eta^{3m} \end{bmatrix} \quad (8)$$

Because of the  $D_{6h}$  symmetry, there are only four different kinds of bond lengths ( $L_a \sim L_d$ ), see Fig.2. The corresponding nearest hopping integrals are  $t_i = t_0 - \alpha(L_i - L_0)$  ( $i = a \sim d$ ). The energy eigenvalues  $E_{pm}^l$  are determined by

$$\lambda^3 + A\lambda^2 + B\lambda + C = 0$$

where

$$\begin{aligned} A &= 2t_a \cos \frac{m\pi}{3} + (-1)^m p t - d, \\ B &= 2 \cos \frac{m\pi}{3} [(-1)^m p t_a t_d - t_c^2] - (2t_c^2 + t_b^2), \\ C &= -4 \cos \frac{m\pi}{3} (1 + \cos \frac{m\pi}{3}) t_a t_c^2 - (-1)^m p t_b^2 t_d \end{aligned}$$

Equation(9) can be solved analytically, so does the eigenvectors. Here we would not list the complicated analytical results. Instead, we present numerical results by using parameters sets,  $t_a = 3.30\text{eV}$ ,  $t_b = 2.95\text{eV}$ ,  $t_c = 3.24\text{eV}$ ,  $t_d = 3.08\text{eV}$ , which are determined by the bond lengths  $L_i$ . The coefficients  $c_{mp,l}^i$  of the energy eigenstate wavefunction  $\Phi_{mp}^i$  and their irreducible representations of  $D_{6h}$  that they belong to are showed in Table 1.

In the  $C_{36}$  molecule, because the hexagons in two middle layers turn an angle of  $30^\circ$  to the four hexagons at two ends, the wavefunctions of  $B_{2u}$  and  $B_{1g}$  energy eigenstates

are entirely composed of the atom orbits on the two middle layers, while those of  $B_{1u}$  or  $B_{2g}$  energy eigenstates only have amplitude on the other four layers. There are six energy eigenstates of the B kind representations. The 13th( $B_{2u}$ ), 22nd( $B_{1g}$ ), the accidentally degenerate 35th( $B_{1u}$ ) and 36th( $B_{2g}$ ) levels lie either far below or above the fermi level, so they are of no interest. There are also another pair of accidentally degenerate 18th( $B_{1u}$ ) and 19th( $B_{2g}$ ) levels which are half filled. We also notice in Table 1. that the 18th( $B_{1u}$ ) and 19th( $B_{2g}$ ) electrons are distributed in the 2nd and 5th layers with 90% possibility and 10% in the 1st and 6th layers.

When  $t_1(16.8\%t_0)$  and  $t_2(11.1\%t_0)$  are considered,  $H_{mp}$  have a different form. The long distance hopping( $t_2$ ) coupling the 2nd and 5th layers results in  $B_{1u}$  and  $B_{2g}$ 's splitting. This is the reason that we introduce much longer distance hopping term than usual. Because the charge densities of  $B_{1u}$  and  $B_{2g}$  are mainly distributed in the 2nd and 5th layers, the gap between HOMO( $B_{1u}$ ) and LUMO( $B_{2g}$ ) is approximately  $2t_2$ . When the electron-electron interaction is taken into account, the electronic Hamiltonian has to be solved in the HF mean field theory with self-consistent method. The energy levels of ground state configuration are shown in Fig.3. We can see that in Fig.3 and Table 1, the relative positions of the energy levels only change slightly, except the splitting of  $B_{1u}$  and  $B_{2g}$ . In Fig.2, the separation between the 16th, 17th levels( $E_{1g}$ ) and HOMO is about 0.2eV and that between the 20th, 21st levels ( $E_{2g}$ ) and LUMO is 1.3eV.

#### IV. NUMERICAL RESULT OF THE MOLECULE

Under the adiabatic approximation, we apply the BdeG formalism to the Hamiltonian of the molecule to obtain the stable lattice configuration and the corresponding electronic structure. Molecular dynamic procedure is used to gradually approach the minimum of the potential surface from an initial lattice configuration. The following two equations are used,

$$F_{i\sigma} = -\frac{d V_{eff}}{d x_{i\sigma}} \quad (\sigma = 1 - 3) \quad (9)$$

$$v_{i\sigma} = \frac{d x_{i\sigma}}{d t} \quad (10)$$

where  $V_{eff}$  is the effective lattice potential that includes the elastic energy of the lattice and the electron-lattice interaction energy, both of which depends on the lattice coordinates.  $F_{i\sigma}$  is the  $\sigma$  component of the effective force acted on the  $i$ th atom under this potential.  $x_{i\sigma}$  is the  $\sigma$  coordinate of the  $i$ th atom.

In each step of the dynamical procedure, we solve the electrical part of the Hamiltonian under the lattice configuration given by the last step. The HF mean field theory is performed to decouple the electron-electron interaction. Then the electronic states and wavefunctions are obtained self-consistently.

$$\begin{aligned} H_{MF}^{el} = & H_0 + U \sum_i \{ \langle n_{i\uparrow} \rangle n_{i\downarrow} + \langle n_{i\downarrow} \rangle n_{i\uparrow} - \langle n_{i\uparrow} \rangle \langle n_{i\downarrow} \rangle \} \\ & + V \sum_{\langle i,j \rangle, \sigma, \sigma'} \{ \langle n_{i\sigma} \rangle n_{j\sigma'} + \langle n_{j\sigma'} \rangle n_{i\sigma} - \langle n_{i\sigma} \rangle \langle n_{j\sigma'} \rangle \} \\ & - V \sum_{\langle i,j \rangle, \sigma} \{ \langle C_{i\sigma}^\dagger C_{j\sigma} \rangle C_{j\sigma}^\dagger C_{i\sigma} + \langle C_{j\sigma}^\dagger C_{i\sigma} \rangle C_{i\sigma}^\dagger C_{j\sigma} - \langle C_{i\sigma}^\dagger C_{j\sigma} \rangle \langle C_{j\sigma}^\dagger C_{i\sigma} \rangle \} \end{aligned} \quad (11)$$

The ground state and the lowest triplet and singlet excitons are investigated. There are four lowest exciton configurations  $A, B, C$  and  $D$ , see Fig. 4. Due to Coulomb interaction,  $C$  and  $D$  are mixed to give singlet and triplet,

$$\begin{aligned} \langle C | H_{int} | D \rangle = & - \sum_i U \psi_{\alpha\uparrow}^*(i) \psi_{\beta\downarrow}^*(i) \psi_{\beta\uparrow}(i) \psi_{\alpha\downarrow}(i) \\ & - V \sum_{\langle ij \rangle} \{ \psi_{\alpha\uparrow}^*(i) \psi_{\beta\downarrow}^*(j) \psi_{\beta\uparrow}(i) \psi_{\alpha\downarrow}(j) + \psi_{\alpha\uparrow}^*(j) \psi_{\beta\downarrow}^*(i) \psi_{\beta\uparrow}(j) \psi_{\alpha\downarrow}(i) \} \end{aligned} \quad (12)$$

where  $\alpha$  and  $\beta$  denote the 18th and 19th energy level respectively.

## V. RESULTS AND DISCUSSION

The configurations and energy of ground and low excited states are given below,

$$E_1^{el} = -64.25 \text{ eV} \quad |\Phi_1\rangle \text{ (spin singlet ground state)}, \quad (13a)$$

$$E_2^{el} = -64.00 \text{ eV} \quad |\Phi_2^{1\sim 3}\rangle = |A\rangle, |B\rangle, \frac{1}{\sqrt{2}}(|C\rangle + |D\rangle) \text{ (spin triplets)}, \quad (13b)$$

$$E_3^{el} = -63.37 \text{ eV}, \quad |\Phi_3\rangle = \frac{1}{\sqrt{2}}(|C\rangle - |D\rangle) \text{ (spin singlet)}. \quad (13c)$$

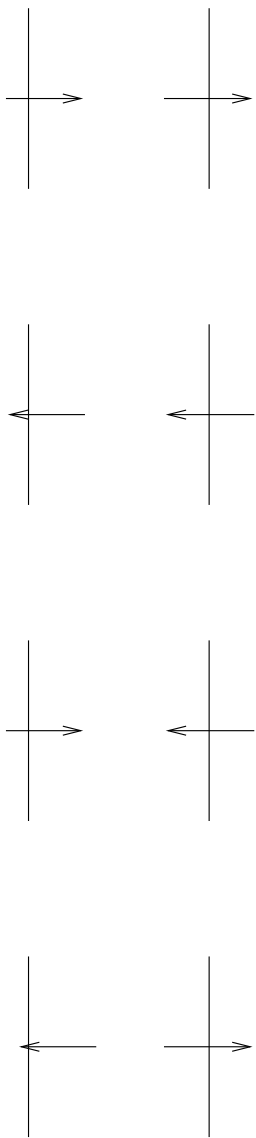


FIG. 4. The four possible configurations of the lowest excitons.

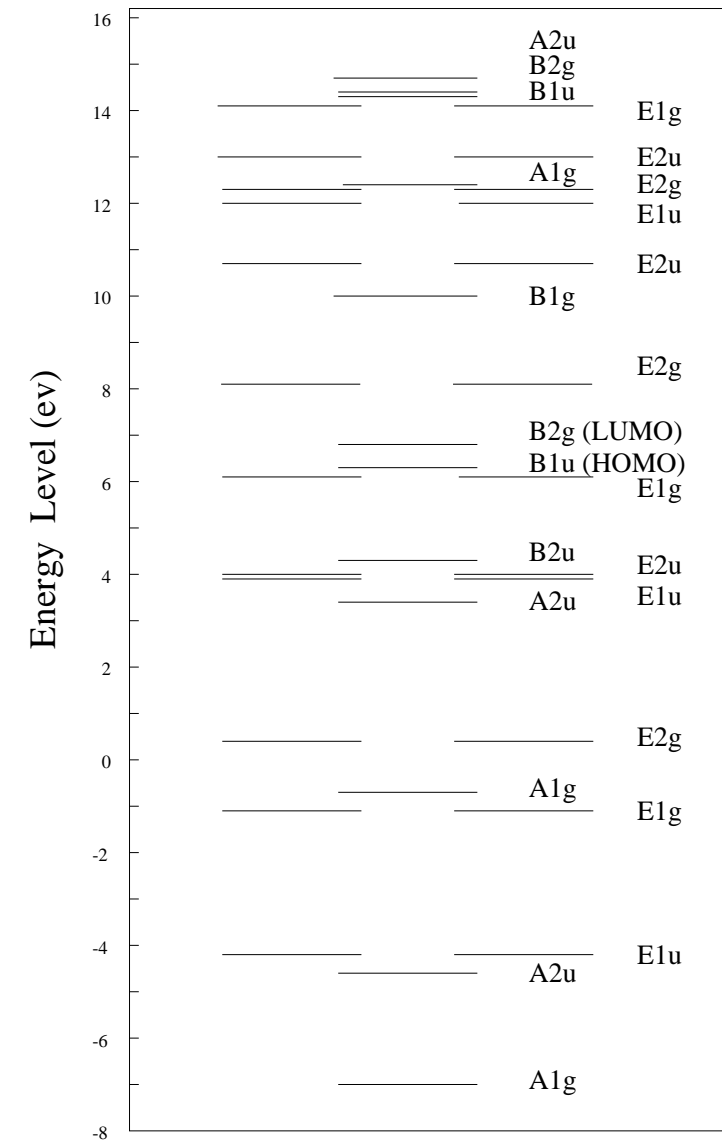


FIG. 3. Energy levels of the ground state C<sub>36</sub> molecule.

	1	2	3	4	5	6
$C_{36}^{2-}$	1.053	1.131	0.991	0.991	1.131	1.053
$C_{36}^-$	1.042	1.057	0.985	0.985	1.057	1.042
$C_{36}$	1.031	0.981	0.988	0.988	0.981	1.031
$C_{36}^+$	1.021	0.902	0.992	0.992	0.902	1.021
$C_{36}^{2+}$	1.013	0.823	0.997	0.997	0.823	1.013

TABLE II. The ground state charge density per site on each layer of ions and molecule.

We can see that the ground state  $\Psi_1$  is a spin singlet rather than triplet after the long distance hopping  $t_2$  and electron-electron interaction are taken into account, which is an improvement of the prediction of simple Hückel theory, and there is no need to add the hybridizing of  $\sigma$  and  $\pi$  bonds to investigate the qualitative physics of  $C_{36}$  as discussed in Ref. [8].

The lowest excited states  $\Psi_2^{1-3}$  are spin triplet excitons, which are only about 0.25eV above the ground states. The energy of singlet exciton  $\Psi_3$  is very high, and the splitting between the triplet and singlet excitons is about 0.63eV, which is much larger than 0.2eV in the cases of  $C_{60}$  and  $C_{70}$ . This is because the electrons of HOMO and LUMO are more localized, 90% in the 2nd and 5th layers and 10% in the 1st and 6th layers. Compared to the  $C_{36}$  case, the electron densities of HOMO and LUMO in  $C_{60}$  and  $C_{70}$  are distributed more uniformly over all sites, so the splitting of the singlet and triplet exciton due to the Coulomb interaction is relatively small. The fact that the triplet exciton has low energy can be verified through experiment observation: When illuminated by external light, the  $C_{36}$  can be excited to the state of singlet exciton and then may transit to triplet exciton through nonradiative decay. The transition rate to ground state is slow because of the different spin configuration and small energy splitting. We predict that the triplet excitons are metastable states, and the phosphorescence phenomena is possible to be observed. The

	$L_1$	$L_2$	$L_3$	$L_4$
SSH( $C_{36}^{2-}$ )	1.414	1.453	1.418	1.447
SSH ( $C_{36}^-$ )	1.410	1.462	1.418	1.447
SSH( $C_{36}$ )	1.407	1.470	1.418	1.447
SSH( $C_{36}^+$ )	1.404	1.477	1.417	1.447
SSH( $C_{36}^{2+}$ )	1.402	1.484	1.417	1.448
LDA( $C_{36}$ )	1.41	1.48	1.43	1.43

TABLE III. The bond length(Å) of ions and molecule.

	$\alpha$	$\beta$	$\gamma$	$\delta$	$\varepsilon$	$\phi$
$C_{36}$	120.00°	107.64°	108.20°	108.29°	119.42°	119.24°

TABLE IV. The bond angle within SSH model.

triplet exciton is paramagnetic while the ground state is a diamagnetic singlet. So the magnetic susceptibility is increased upon illumination of the external light. Electron Spin Resonance(ESR) experiment can be performed to detect the triplet exciton states. When ESR is performed to a solution sample, the usual unimportant magnetic dipole interaction between electrons becomes crucial because its anisotropy can smear the resonance peak. However, this interaction is decayed rapidly with distance as  $R^{-3}$ . The electrons in HOMO and LUMO are mainly uniformly distributed on 12 carbon atoms in two layers, the possibility of their short distance is considerably small compared to other small organic molecule, such as naphthalene. So the resonance peak is possible to be observed. The phone absorption and luminescence spectra experiments can be perform to test the lowest singlet exciton's energy.

The shape of the  $C_{36}$  molecule is an ellipsoid with high aspect ratios. Our calculation shows that the distance between the 1st and 6th layers is  $5.2A^\circ$ , and that between the parallel vertical hexagon planes is  $4.2A^\circ$ . The charge density, bond lengths and bond angles of  $C_{36}$  molecule and ions are calculated and shown in Table 2, 3 and 4. We note that because of the  $D_{6h}$  symmetry of the molecule, the 1st and 6th layers are regular hexagons, with each internal angle  $120^\circ$  and the shortest bonds ( $L_1$ )  $1.41A^\circ$ . The six vertical hexagons around the equator are slightly deformed due to the drag of the 1st and 6th layers from each side.  $L_4$  is 2.8% longer than  $L_1$  and 2% than  $L_3$ . The  $L_2$  bonds are relatively weaker than those in hexagons, because they couple the hexagons in the two ends with the hexagons around the equator.  $L_2$  is 4.4% longer than  $L_1$ . This result is consistent with that of LDA except that the  $L_4$  is as long as  $L_3$  in LDA, and we think that our result is more reasonable.

The bond lengths of  $L_3$  and  $L_4$  of ions differ from those of molecule very slightly. But the negative polarons'  $L_1$  is longer and positive polaron' is shorter than the neutral molecule's, while the  $L_2$  changes in the opposite way.

The reason is that the wavefunctions of the electron in  $B_{1u}$  and  $B_{2g}$  has opposite sign between two nearest sites connected by  $L_1$ , same sign by  $L_2$ , and have zero amplitude on the 3rd, 4th layers. According to the contribution f these two states form hopping term, the sites connected by  $L_1$  are repulsive, but those connected by  $L_2$  are attractive. The angles in the pentagons and hexagons around the equator deviate from  $108^\circ$  and  $120^\circ$  slightly, which justifies the validity of  $H_{elas}$ . The bond angles in polarons differ from those of molecule very slightly, so we omit them in Table 4. Form  $C_{36}^{2+}$  polaron to  $C_{36}^{2-}$ , the adding electrons distribute mostly in the 2nd and 5th layers. This is because of the particular charge density distribution of the 18th and 19t levels.

## VI. CONCLUSION

In this paper, we have carefully studied the effect of  $D_{6h}$  symmetry on  $C_{36}$ 's electronic properties under the extended SSH model. A small gap between  $HOMO(B_{2u})$  and

LUMO( $B_{1g}$ ) is obtained due to long distance hopping. The large splitting of the spin triplet and singlet lowest excitons, the differences of bond lengthes and electron density between molecule and polarons are discussed as results brought by the more localized HOMO and LUMO and their special symmetries. Possilbe experiments are suggested.

#### **ACKNOWLEDGMENT**

We thank Dr. Xi Dai for his helpful discussions.

## REFERENCES

- [1] C.Piskoti, J.Yarger, A. Zettl, *Nature* **393**, 771(1998).
- [2] M.Cote J.C.Grossman, S.G.Louie, M.L.Cohen *Phy. Rev. Lett* **81**, 697(1998)
- [3] J.C.Grossman, M.Cote, S.G.Louie, M.L.Cohen *Chem. Phys. Lett.* **284**, 344(1998)
- [4] W.M.You, C.L.Wang, F.C.Zhang, Z.B.Su, *Phy.Rev.B* **47**, 4765(1993)
- [5] L. Tian, Y.S.Yi, C.L.Wang, Z.B.Su, *Int.Jou.Mod.Phys.B* **11**, 1969(1997)
- [6] C.L.Wang, W.Z.Wang, Z.B.Su, *J.Phys.Condes.Matter* **5**, 5581(1993)
- [7] Y.Deng, C.N.Yang, *Phys.Lett.A* **170**, 116(1992)
- [8] J.R.Heath, *Nature* **393**, 730(1998)